Available online at www.sciencedirect.com
ScienceDirect
Energy Reports 7 (2021) 97–103
www.elsevier.com/locate/egyr

5th Annual CDT Conference in Energy Storage and Its Applications, Professor Andrew Cruden, 2021, 07–19, University of Sheffield, U.K.

Estimating lithium-ion battery behavior from half-cell data

Ben Rowden*, Nuria Garcia-Araez

Chemistry, University of Southampton, University Road, Highfield, Southampton, SO17 1BJ, UK

Received 17 February 2021; accepted 17 February 2021

Abstract

The electrochemical behavior of lithium-ion battery electrode materials is often studied in the so-called 'lithium half-cell configuration', in which the electrode is tested in an electrochemical cell with a lithium metal electrode acting as both counter and reference electrode. However, the performance of lithium-ion batteries is affected by the electrochemical behavior of the two electrodes composing the battery. Therefore, in order to understand the behavior of battery materials under conditions representative of commercial applications, it is necessary to perform electrochemical measurements in the so-called 'full-cell configuration', in which a cathode (e.g. lithium iron phosphate or LFP) and an anode (e.g. graphite) are combined in an appropriate capacity ratio. In this work, we provide further understanding of how the behavior of the electrodes in half-cell configuration affects the electrochemical response of the full cell. For that, we characterize two commercially relevant battery materials, LFP and graphite, in lithium half-cells, and also combined in a LFP vs graphite full-cell. Additionally, we employ the electrochemical response of the LFP and graphite electrodes in lithium-half cells to predict the electrochemical response of the LFP vs graphite full-cell, and the results of our calculations are in very good agreement with the experimental measurements.

Peer-review under responsibility of the scientific committee of the 5th Annual CDT Conference in Energy Storage and Its Applications, Professor Andrew Cruden, 2021.

Keywords: Lithium ion; Battery; Half-cell; Full-cell

1. Introduction

Lithium-ion batteries are one of the most commonly used energy storage technologies with applications in portable electronics and electric vehicles. Characteristics such as high energy density, good cycling ability, high operating voltage and low self-discharge are pivotal in making lithium-ion batteries the leading technology for these applications. Their unquestionable commercial success has promoted a huge amount of research dedicated to achieve even further improvements in areas such as energy density, degradation, cycle life and safety [1,2].

The investigation of lithium-ion battery electrode materials is often made in lithium half-cell configurations, where a lithium metal electrode is utilized as both the counter and reference electrode. Lithium metal is used for that purpose because it provides a stable reference potential and has a large specific capacity of 3860 mA h g^{-1},

* Corresponding author.
E-mail address: b.rowden@soton.ac.uk (B. Rowden).

https://doi.org/10.1016/j.egyr.2021.02.048

Peer-review under responsibility of the scientific committee of the 5th Annual CDT Conference in Energy Storage and Its Applications, Professor Andrew Cruden, 2021.

which affords a very large reservoir of capacity so that the reactions at the working electrode are not limited by the capacity available at the counter electrode [3]. (For example, for the lithium thickness of 100 μm used here, the areal capacity is ca. 20.6 mA cm^{-2}, which is much larger than the < 5 mA cm^{-2} of typical battery electrodes [4]). Thus, the characterization of lithium-ion battery electrodes in lithium half-cells is very useful to study the intrinsic electrochemical properties of the materials, but it does not directly predict the behavior of full-cells, composed of a lithium-ion battery cathode and a lithium-ion battery anode, which are used commercially

Full-cells are constructed by balancing the capacity of the cathode and anode to make them similar. Specifically, commercial lithium-ion cells are made with anodes that have somewhat higher capacity (around 10%) than the cathodes, with the purpose of preventing lithium plating on the graphite anode [5]. Consequently, when charging the cell, the full-cell capacity is limited by the cathode. However, in this process of charging, a limited capacity is inserted in the anode, and therefore, on the subsequent discharge, the full-cell capacity is limited by the anode. Furthermore, since capacity-consuming side-reactions take place on charge (like the formation of a solid electrolyte interphase, SEI, on graphite [6]) then the capacity available for discharge is smaller than the capacity spent on charge. This loss of capacity due to side-reactions (usually called 'loss of cyclable lithium') is unfortunate, and, albeit in smaller extent, continues in further cycles and it is, indeed, the predominant mechanism of capacity loss [7,8].

In this work, we bring further understanding on the electrochemical behavior of full-cells, by quantitatively analyzing and comparing experimental data of half-cells and full-cells. We present a simple method of calculation that enables us to predict the behavior of the full-cell, based on half-cell data, as well as predicting and quantifying the loss of capacity of full-cells due to the mechanism of loss of cyclable lithium described above. We illustrate our analysis using lithium iron phosphate (LFP) and graphite as battery materials, due to their importance for commercial applications [9].

2. Experimental

2.1. Electrode production

Lithium iron phosphate (LFP, Tatung) and graphite (Hitachi, mage 3) electrodes were produced by mixing the active material, polyvinylidene fluoride (PVDF 5130, Solvay) and Super C65 conductive carbon (Timcal) in a mass ratio of 92:4:4 for LFP electrodes and 94:3:3 for graphite electrodes. A viscous ink was produced by mixing the electrode components and N-methyl-2-pyrrolidone (NMP, Sigma-Aldrich, anhydrous 99.5%) with a volume of solvent of 1.65 ml of NMP per 1 g of solid. The ink was mixed for 3 sets of 5 min at 2000 rpm with 5-minute rest steps in between in a planetary mixer (Thinky). LFP slurries were coated onto 99% purity 0.035 mm thick aluminium foil (Advent) at a wet thickness of 420 μm using a doctor blade (TQC Sheen). Graphite slurries were coated onto 99% purity 0.05 mm thick copper foil (Advent) at a wet thickness of 300 μm using a doctor blade (TQC Sheen). All electrode sheets were dried in a vacuum oven for 4 h at 80 °C. Electrodes were punched using a precision punch (Nagomi) at a diameter of 24 mm for LFP electrodes and 25 mm for graphite electrodes. All electrodes were compressed using a pellet press (Specac) at 5 tonnes. The electrodes were dried overnight under vacuum in a Buchi tube at 120 °C prior to introduction into a glovebox.

2.2. Electrochemical testing

Electrochemical testing of both LFP and graphite electrodes was carried out using 316 stainless steel union cells (Swagelok) of one-inch inner diameter, lined with fluorinated ethylene propylene (FEP) film. All cells were assembled in an argon glovebox (Labstar, MBraun) with H_2O and O_2 <0.1 ppm. Both half-cell configurations were assembled by stacking a 100 μm thick, 25 mm diameter lithium metal electrode (Rockwood lithium) onto a copper current collector. On top of the lithium metal, two 25 mm diameter GF/F (Whatman, 0.4 mm thick, 0.7 μm pore size) separators were placed. 700 μl of 1 M $LiPF_6$ in ethylene carbonate (EC) and ethylene methyl carbonate (EMC) with (EC:EMC 3:7 weight ratio) (LP57, PuriEL, Soulbrain) was then pipetted onto the separator, and then LFP or graphite was placed on top. The cell assembly was completed with insertion of a current collector cap, spring and a current collector. For LFP these components were made of aluminium, for graphite electrodes they were made of copper.

Full-cells of LFP vs graphite were assembled using the same procedure as LFP half-cells, with the graphite electrode replacing the lithium metal disc. Capacity balancing was done by using a graphite electrode with a

10% higher areal capacity than the LFP electrode. The specific capacities used for full-cell balancing and for the calculation of C-rates were 155 mA h g^{-1} for LFP and 370 mA h g^{-1} for graphite. The electrodes used in the full-cell experiments had active material loadings of 12.36 mg_{LFP} cm^{-2} for LFP (corresponding to an areal capacity of 1.92 mA h cm^{-2} based on a specific capacity of 155 mA h g_{LFP}^{-1}) and 5.83 mg_C cm^{-2} for graphite (corresponding to an areal capacity of 2.16 mA h cm^{-2} based on a specific capacity of 155 mA h g_{LFP}^{-1}). In the half-cell experiments, the electrodes had an active material loading of 12.62 mg_{LFP} cm^{-2} for LFP and 5.48 mg_C cm^{-2} for graphite. Ten repeats of the full-cell experiments were done to evaluate the reproducibility. The active material loadings were in the range of 12–13 mg_{LFP} cm^{-2} for LFP and 5.5–6 mg_C cm^{-2} for graphite. Four repeats of the half-cell experiments were also done, and the active material loading ranged between 13–14 mg_{LFP} cm^{-2} for LFP and 4.5–5.5 mg_C cm^{-2} for graphite.

After assembly, the cells were placed inside a climactic chamber (Memmert) set to 25 °C. Electrochemical testing was done via Galvanostatic cycling at C/20, with the voltage ranges for the three cell configurations being: LFP vs. Li: 2.7–4.1 V, Graphite vs. Li: 0.005–1.5 V, LFP vs. Graphite: 2.2–4.1 V.

3. Data analysis and results

Fig. 1 hows the results of the electrochemical characterization of LFP and graphite electrodes in lithium half-cells, and the values of specific capacities are shown in Table 1. The shape of the voltage profiles, high specific capacities and high coulombic efficiencies are consistent with previous work [6,10]. The electrochemical half-cell data was then employed to predict the behavior of full-cells made of LFP vs graphite. Fig. 2 shows the comparison between the predicted (calculated) behavior of the full-cell and the experimentally obtained one. The identification of the limiting electrode and the reactions involved in the full cell are shown in Fig. 3.

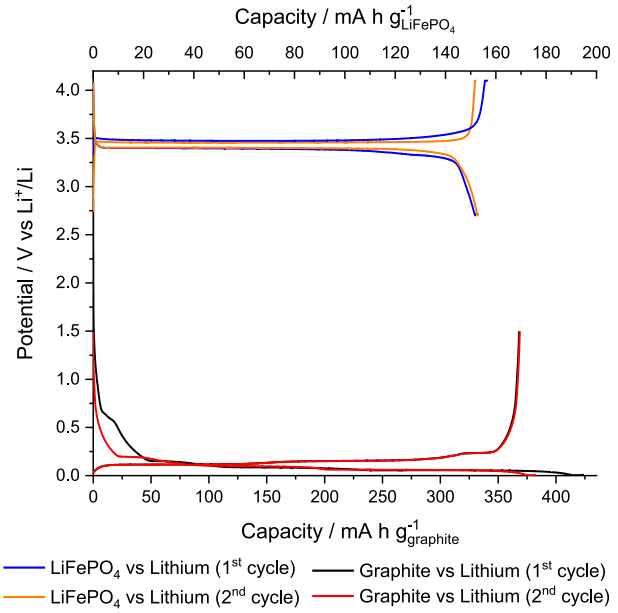

Fig. 1. Typical potential profile of a $LiFePO_4$ vs lithium half-cell (2.7 V–4.1 V) and a separate graphite vs lithium half-cell (0.005 V–1.5 V) in the first two cycles at C/20.

Table 1. Experimental specific capacities of $LiFePO_4$ and graphite electrodes tested in lithium half-cells at C/20 (data shown in Fig. 1). Error values reflect a confidence interval at 95% confidence level calculated from four repeat measurements.

	Graphite capacity/mA h g_C^{-1}	$LiFePO_4$ capacity/mA h g_{LFP}^{-1}
1st charge	423 ± 10	157 ± 1
1st discharge	368 ± 9	152 ± 1
2nd charge	382 ± 4	152 ± 1
2nd discharge	369 ± 3	152 ± 2

Table 2. Experimental and calculated specific capacities of a $LiFePO_4$ vs graphite full-cell cycled at C/20 (data shown in Fig. 2). Error values for the experimental values reflect a confidence interval at 95% confidence level calculated from ten repeat measurements. For the calculated values the error is calculated via the propagation of errors throughout the calculation. For simplicity, the values of capacity are normalized to the mass of graphite active material only.

	Calculated $LiFePO_4$ vs graphite cell capacity/mA h g_C^{-1}	Experimental $LiFePO_4$ vs graphite cell capacity/mA h g_C^{-1}
1st charge	341 ± 2	330 ± 3
1st discharge	286 ± 6	288 ± 4
2nd charge	286 ± 7	290 ± 4
2nd discharge	273 ± 7	273 ± 4

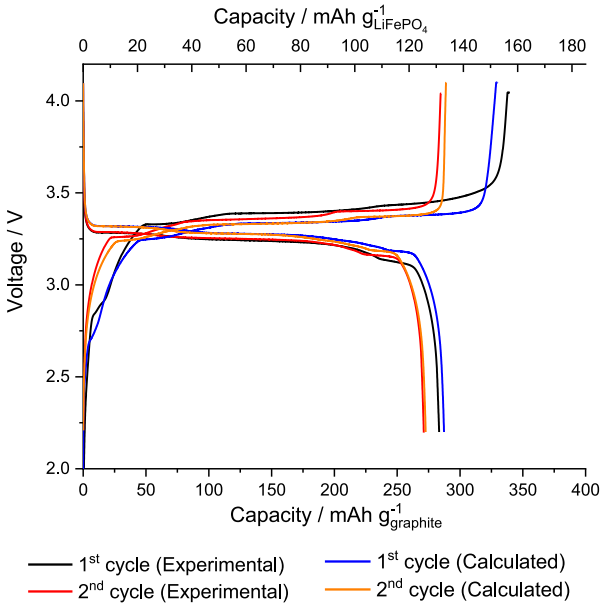

Fig. 2. Comparison of experimental and calculated voltage profiles of a $LiFePO_4$ vs graphite full-cell cell, in the first two cycles at C/20 in the voltage range of 2.2 V–4.1 V. The calculated voltage profile was produced from the data in Fig. 1.

The predictions of the LFP vs graphite full-cell behavior were done as follows. In the first charge, the capacity of the full-cell is limited by the LFP electrode, which is able to deliver 157 ± 1 mA h g_{LFP}^{-1}. Due to the capacity balancing employed for building our LFP vs graphite full-cell, this value of capacity of the LFP electrode corresponds to a capacity of 341 ± 2 mA h g_C^{-1} when normalized by the mass of the graphite active material [Note that the ratio of LFP and graphite loadings is 370/(155*1.1) $g_{LFP}\ g_C^{-1} = 2.17\ g_{LFP}\ g_C^{-1}$]. Therefore, the prediction of the full-cell behavior from half-cell data is that the full-cell achieves a capacity of 157 ± 1 mA h g_{LFP}^{-1} or 341 ± 2 mA h g_C^{-1} in the first charge (Table 2). Experimentally, a first charge capacity of 152 ± 2 mA h g_{LFP}^{-1} or 330 ± 3 mA h g_C^{-1} is obtained (Table 2), in reasonably good agreement with the predictions from calculations.

The evaluation of the voltage profile of the full-cell in the first charge is simply done by noting that the cell voltage is the difference in potential of the LFP and graphite electrodes (where the values of potential of each individual electrode are obtained from the lithium half-cell measurements in Fig. 1) for each value of capacity (not specific capacity) in the full-cell. For example, for the active material loadings used here in the full-cell, an areal capacity of 0.01 mA cm^{-2} for the full cell corresponds to specific capacity values of 0.809 mA h g_{LFP}^{-1} for LFP and 1.715 mA h g_C^{-1} for graphite. In practice, the calculation was done by interpolating constant values of full-cell capacity, and obtaining the corresponding values of potential of LFP and graphite electrodes from the half-cell data. Fig. 2 shows the comparison of the calculated (blue curve) and experimental (black curve) full-cell voltage profiles in the first charge, showing very good agreement.

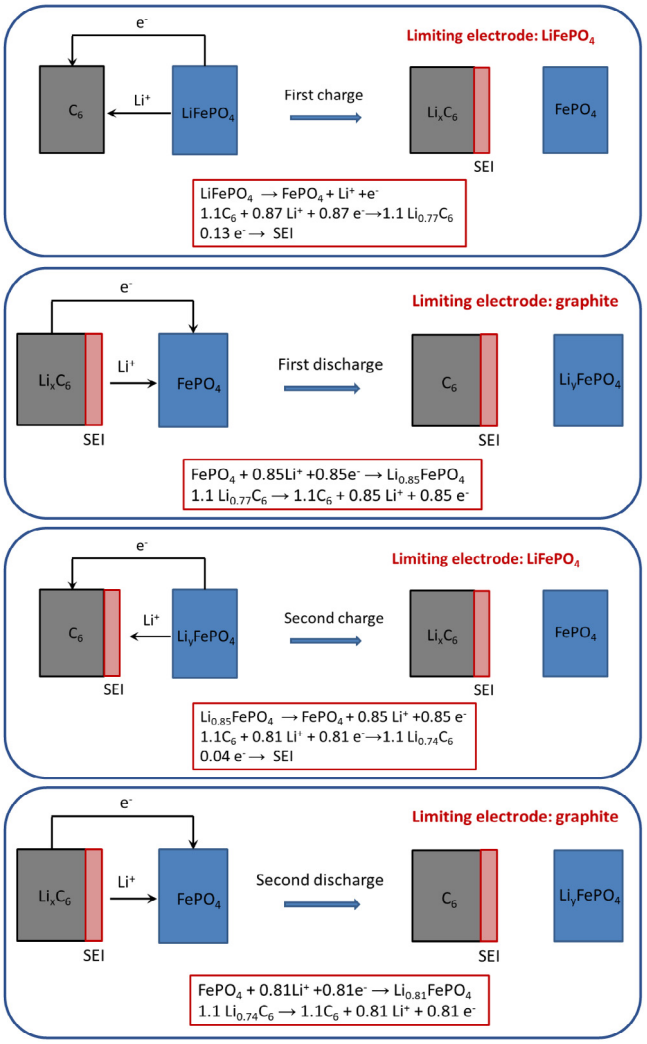

Fig. 3. Diagrams and equations representing the reactions involved in full-cells of LFP vs graphite in the first two charge/discharge cycles. The first charge capacity of the full cell is limited by the lithium content of the $LiFePO_4$ with a capacity of 157 mA h g_{LFP}^{-1} = 341 mA h g_c^{-1}. The irreversible capacity loss in the first cycle of graphite in a half-cell is 55 mA h g_c^{-1}. Therefore, the amount of lithium inserted in graphite at the end of the first full-cell charge is $x = (341 - 55)/370 = 0.77$. After that, in the first discharge of the full-cell, the limiting electrode is the lithiated graphite, which delivers the capacity associated with the lithium that was inserted on the first charge: (341–55) mA h g_c^{-1} = 286 mA h g_c^{-1} = 132 mA h g_{LFP}^{-1}. Consequently, the amount of lithium inserted in $FePO_4$ in the first discharge is $y = 132/155 = 0.85$. After that, in the second charge, the full-cell capacity is limited by the Li_yFePO_4 electrode, which provides the capacity that it received on the first discharge: 132 mA h g_{LFP}^{-1} = 286 mA h g_c^{-1}. The irreversible capacity loss of graphite in a half-cell in the second cycle is 13 mA h g_c^{-1}. Therefore, the amount of lithium inserted in graphite at the end of the second charge is $x = (286 - 13)/370 = 0.74$. Finally, in the second discharge of the full-cell, the limiting electrode is the lithiated graphite, which delivers the capacity associated with the lithium that was inserted on the second charge: 286–13 mA h g_c^{-1} = 273 mA h g_c^{-1} =126 mA h g_{LFP}^{-1}. Consequently, the amount of lithium inserted in $FePO_4$ in the second full-cell discharge is $y = 126/155 = 0.81$.

The assessment of the voltage profile of the full-cell in the subsequent discharge needs to take into account that the capacity is limited by the amount of lithium that was inserted in graphite in the previous charge. The capacity in the previous charge is 341 ± 2 mA h g_C^{-1}, when normalized by the mass of the graphite, but part of this capacity is consumed in side-reactions (e.g. the formation of a solid electrolyte interphase, SEI), rather than the insertion of lithium in graphite. The half-cell data of graphite shows that the irreversible specific capacity (that is, the difference in the lithiation and de-lithiation specific capacities) in the first cycle is 423–368 mA h g_C^{-1} = 55 mA h g_C^{-1}.

Consequently, of the total capacity of 341 mA h g_C^{-1} spent on charge, only 341–55 mA h g_C^{-1} = 286 mA h g_C^{-1} is spent in lithium insertion in graphite. Therefore, the capacity that is available in the discharge of the full-cell is only 286 ± 6 mA h g_C^{-1}, corresponding to 132 ± 3 mA h g_{LFP}^{-1} when normalized by the mass of LFP. [Note that the error is calculated from the propagation of errors from the experimental half-cell data]. As shown in Table 2, these predictions from half-cell data match well with what is obtained experimentally in the full-cell.

The calculation of the full-cell voltage profile during discharge needs to consider the capacity loss due to side-reactions on graphite on charge. The graphite half-cell data has a specific first discharge capacity of 368 mA h g_C^{-1}, but the discussion above shows that only 286 mA h g_C^{-1} are available in the full-cell cycling. Therefore, it is necessary to subtract 368–286 mA h g_C^{-1} = 82 mA h g_C^{-1} from the potential vs capacity curve of graphite in half-cells to perform the calculations of the voltage profile in the full-cells. As shown in the comparison of calculations and experiments in Fig. 2 (blue and black curves), the first discharge profiles are in good agreement.

In the second charge, the full-cell capacity is limited by the lithium that has been inserted in $FePO_4$ in the previous discharge, which corresponds to 132 ± 3 mA h g_{LFP}^{-1} when normalized by the mass of LFP, and 286 ± 6 mA h g_C^{-1} when normalized to the mass of graphite. Table 2 shows, again, good agreement with experiments. For the calculation of the full-cell voltage profile, it needs to be taken into account that the beginning of the second charge does not start with a fully lithiated $LiFePO_4$, but with a partially-delithiated Li_yFePO_4 that only contains 132 mA h g_{LFP}^{-1} of capacity of inserted lithium. Since the half-cell data of the second charge of $LiFePO_4$ exhibits a capacity of 152 mA h g_{LFP}^{-1}, it is necessary to subtract 152–132 mA h g_{LFP}^{-1} = 20 mA h g_{LFP}^{-1} in order to obtain the potential vs capacity curve to use for the full-cell voltage calculations. The comparison of the calculated and experimental voltage profiles in Fig. 2 (orange and red curves, respectively) again show very good agreement.

Finally, in the second discharge of the full-cell, it needs to be taken into account that the graphite electrode again underwent a capacity loss in the previous charge, and therefore, not all the full-cell capacity on charge is available for discharge. In the graphite half-cell, the irreversible capacity in the second cycle is 369–382 mA h g_C^{-1} = 13 mA h g_C^{-1}. Consequently, of the total capacity of 286 mA h g_C^{-1} spent on charge, only 286–13 mA h g_C^{-1} = 273 mA h g_C^{-1} is spent in lithium insertion in graphite. Therefore, the capacity that is available in the discharge of the full-cell is only 273 ± 7 mA h g_C^{-1}, corresponding to 126 ± 3 mA h g_{LFP}^{-1} when normalized by the mass of LFP. As shown in Table 2, the predictions from calculations and the experimental results are again in good agreement.

For the calculation of the full-cell voltage on the second discharge, it is necessary to consider the capacity loss due to side-reactions. The graphite half-cell data has a specific second discharge capacity of 369 mA h g_C^{-1}, but the discussion above shows that only 273 mA h g_C^{-1} is available in the full-cell cycling. Therefore, it is necessary to subtract 369-273 mA h g_C^{-1} = 96 mA h g_C^{-1} from the potential vs capacity curve of graphite in half-cells to perform the calculations of the voltage profile in the full-cells. Fig. 2 shows the comparison of the calculated and experimental results (orange and red curves, respectively), showing again good agreement.

Conclusions

In conclusion, we have shown that it is possible to accurately predict the behavior of full-cells by employing data recorded in half-cells, and that these calculations provide a clear and quantitative understanding of the causes of the capacity fade in full-cells. Specifically, the most important cause of capacity fade in the LFP vs graphite full-cells here studied is the loss of cyclable lithium due to side reactions on graphite. The identification of graphite as the main cause of capacity fade is in agreement with previous studies [11,12]. Finally, although procedures for full-cell constructions are well-developed at an industrial scale, the use of full-cells in battery research laboratories is much less common. Therefore, the method of calculation of full-cell behavior from half-cell data here presented can also be used as a method of validation of the full-cell results obtained in a research lab, by using half-cell data that is technically easier to obtain.

Declaration of competing interest

The authors declare that they have no known competing financial interests or personal relationships that could have appeared to influence the work reported in this paper.

Acknowledgments

The authors gratefully acknowledge financial support from the UK Engineering and Physical Sciences Research Council (EPSRC) through the Centre for Doctoral Training in Energy Storage and its Applications (Grant No. EP/L016818/1). We also gratefully acknowledge the reviewer of this article for the excellent suggestions to improve the quality and clarity of the article.

References

[1] Winter M, et al. Insertion electrode materials for rechargeable lithium batteries. Adv Mater 1998;10(10):725–63.
[2] Whittingham MS. Lithium batteries and cathode materials. Chem Rev 2004;104(10):4271–302.
[3] Wood KN, Noked M, Dasgupta NP. Lithium metal anodes: Toward an improved understanding of coupled morphological, electrochemical, and mechanical behavior. ACS Energy Lett 2017;2(3):664–72.
[4] Gallagher KG, et al. Optimizing areal capacities through understanding the limitations of lithium-ion electrodes. J Electrochem Soc 2016;163(2):A138–49.
[5] Son B, et al. Effect of cathode/anode area ratio on electrochemical performance of lithium-ion batteries. J Power Sources 2013;243:641–7.
[6] Wang L, et al. Identifying the components of the solid–electrolyte interphase in Li-ion batteries. Nature Chem 2019;11(9):789–96.
[7] Broussely M, et al. Main aging mechanisms in Li ion batteries. J Power Sources 2005;146(1):90–6.
[8] Smith AJ, et al. Precision measurements of the Coulombic efficiency of lithium-ion batteries and of electrode materials for lithium-ion batteries. J Electrochem Soc 2010;157(2):A196.
[9] Logan ER, et al. Performance and degradation of LiFePO4/graphite cells: The impact of water contamination and an evaluation of common electrolyte additives. J Electrochem Soc 2020;167(13):130543.
[10] Pérez-Rodríguez S, Milton JA, Garcia-Araez N. Novel method of lithium production from brines combining a battery material and sodium sulfite as a cheap and environmentally friendly reducing agent. ACS Sustain Chem Eng 2020;8(16):6243–51.
[11] Shim J, Striebel KA. Cycling performance of low-cost lithium ion batteries with natural graphite and LiFePO4. J Power Sources 2003;119–121:955–8.
[12] Striebel K, et al. The development of low cost LiFePO4-based high power lithium-ion batteries. J Power Sources 2005;146(1):33–8.